OBTAINING MAGNETOCALORIC MnCo(Fe)Ge INTERMETALLICS FROM LOW TEMPERATURE TREATMENT OF MECHANICALLY ALLOYED PRECURSORS

A. Vidal-Crespo , J. J. Ipus , J. S. Blázquez *, and A. Conde

Departamento Física de la Materia Condensada, ICMSE-CSIC, Universidad de Sevilla, P.O. Box 1065, 41080 Sevilla, Spain

*Correspondence: jsebas@us.es

ABSTRACT

Production of the intermetallic $MnCo_{0.8}Fe_{0.2}Ge$ phase, interesting as magnetocaloric material, is obtained by using an almost fully amorphous mechanically alloyed precursor. Thermal treatment to develop the intermetallic phase has been reduced in time (from several hours or even days to few minutes), and temperature (from 1123 K to 723 K). Thermomagnetic measurements allow us to analyze the magnetocaloric effect and to compare the results with those obtained from conventional annealing treatments. Close relationship between magnetocaloric properties and crystal size provides further optimization of the system preserving the advantages of the production method proposed.

Keywords: Magnetocaloric effect, MnCoGe intermetallic, mechanical alloying.

1. Introduction

Energy consumption is a delicate issue in society, consequently, if energy efficiency of cooling systems is improved, it would mean a decrease in the average consumption of each household. Magnetic refrigeration close to room temperature is an useful technology for replacing conventional cooling systems [1]. The target is to find magnetic materials with a large magnetocaloric effect (MCE), which consists in the reversible adiabatic temperature change of a magnetic material upon the application or removal of a magnetic field [2]. To characterize the MCE, the magnetic entropy change, ΔS_M, is widely used, which is related to the temperature change of magnetization, M, by Maxwell relation.

$$\Delta S_M = \mu_0 \int_0^{H_{max}} \left(\frac{\partial M}{\partial T}\right)_H dH \tag{1}$$

where H is the magnetic field and T is the temperature.

Another magnitude for evaluating the performance of a magnetocaloric material is the amount of heat that can be transferred between its cold and hot reservoirs, which is called refrigerant capacity, RC. This magnitude can be defined in three different ways. Firstly, the magnitude can be roughly

approximated to the product of the maximum $\Delta S_M(T)$ curve and the full width at half-maximum (FWHM) of the peak, RC_{FWHM}. Secondly, RC_{AREA} corresponds to the calculation of the area under the curve in the FWHM range. Thirdly, RC_{WP} corresponds to the area of the largest rectangle which can be inscribed under the $\Delta S_M(T)$ curve [3].

Magnetocaloric materials can be classified in terms of the character of the phase transition: a first order magnetostructural/magnetoelastic phase transition (FOPT) or a second order magnetic phase transition (SOPT). On the one hand, materials with a FOPT are characterized by a larger MCE response with respect to SOPT but the sharp character of ΔS_M limits the relevant values to a small temperature range around the transition temperature. Moreover, thermal and magnetic hysteresis phenomena are present, which are disadvantages for their use in cooling devices. On the other hand, there are materials, which present a SOPT with a lower MCE response but broader peaks and without hysteresis phenomena. Independently of the order of the transition, it is important to reduce the concentration of rare earth elements in the system, as it lowers costs and reduces the geopolitical dependence of these elements [4].

Intermetallic compounds with stoichiometry MM'X (where M and M' are transition metals and X is a metalloid), are potential magnetic phase-transition functional materials which present a prominent MCE response. In particular, MnCoGe compounds can exhibit a martensitic transformation from orthorhombic TiNiSi-type structure ($Pnma$ space group) to hexagonal Ni$_2$In-type structure ($P6_3/mmc$ space group) interesting for the ascribed magnetocaloric response [5–7] and the colossal negative thermal expansion [8]. In this system, the MCE response and even the order of the transition can be modified after partial substitution of Fe for Co [5]. However, the formation of the intermetallic phase of interest is not straightforward and long time annealing at high temperatures are needed (typically several days at ~1123 K) [5–7].

Mechanical alloying (MA) technique is widely used to produce supersaturated solid solutions and other metastable systems, including amorphous alloys [9]. Milling metallic powders initially leads to comminution of crystallites, which size is severely reduced to few nanometers (or even leading to amorphization). This supersaturated nanostructure (or amorphous) supplies a short ranged compositionally homogeneous system which is expected to reduce both the temperature and the annealing time needed to produce the intermetallic phase of interest from these precursors. Besides the cost reduction in the annealing process, negative collateral effects such as oxidation would be reduced.

In this work, MnCo$_{0.8}$Fe$_{0.2}$Ge compound was mechanically alloyed starting from a mixture of pure powders to produce a homogeneous system. Microstructure and thermal stability of samples after different milling times were studied. According to their thermal stability, the different samples were

thermally treated and their MCE was studied. Results are compared to those obtained for a sample submitted to a conventional annealing.

2. Experimental

Five grams of high purity (>99%) elements were used in a mixture of nominal composition $MnCo_{0.8}Fe_{0.2}Ge$ (in at. %) was ball milled using steel balls and hardened steel vials in a Fristsch Pulverisette Vario 4 planetary mill. The ball to powder mass ratio was 10:1 and the ratio between the rotational speeds of the vials and the main disk was -2. Continuous milling steps were performed in Ar atmosphere and, after selected times, powder was extracted in a Saffron Omega glove box under Ar atmosphere with oxygen and humidity levels below 2 ppm.

The microstructure was studied by X-ray diffraction (XRD) using a powder diffractometer D8 Advance A25 at room temperature and the radiation employed was $Cu-K_{\alpha}$. The identification of the phases was done using DIFFRAC.EVA software (4.1, Bruker). Quantitative analysis through Rietveld refinement was performed using DIFFRAC.TOPAS software (Version 6, Bruker). Compositions were checked using EAGLE III X-ray microfluorescence equipment. Powder samples were compacted with a hydrostatic press applying 2 tons to obtain disks of ~5 mm diameter. Thermal stability and annealing treatments were performed using a DSC7 Perkin-Elmer calorimeter operating under argon flow. Conventional heat treatments were performed in a GSL1500X oven using samples encapsulated in vacuum in quartz tubes with some Ti threads, which act as oxygen trap to minimize the formation of oxides. Magnetic properties were measured using a Lakeshore 7407 Vibrating Sample Magnetometer (VSM) using a maximum applied field of $\mu_0 H = 1.5$ T. Isothermal magnetization curves were measured from 150 to 350 K with different increments of temperature according to range. Magnetic entropy change was calculated from isothermal magnetization curves using the Maxwell relation performed with the help of the Magnetocaloric Effect Analysis Program [10].

3. Results and Discussion

In order to check the compositional changes during milling due to interaction of the powder with the milling media, composition was checked by X-ray microfluorescence in samples milled 100 h. There are some deviations with respect to the nominal composition as shown in table 1. Mn and Co are reduced with respect to their nominal values (8 and 6 %, respectively) whereas Ge content increases (~12 %). The different capacity of each element to adhere to the milling media can explain this fact: ductile metals and brittle Ge. In the case of Fe the adherence can be compensated by contamination from the steel milling media. No other elements from contamination were detected.

Table 1. Composition observed by X-ray microfluorescence

Element	At. % expected	At. % observed
Mn	33.33	30.8 ± 0.2
Co	26.67	25.0 ± 0.2
Fe	6.67	7.0 ± 0.1
Ge	33.33	37.2 ± 0.3
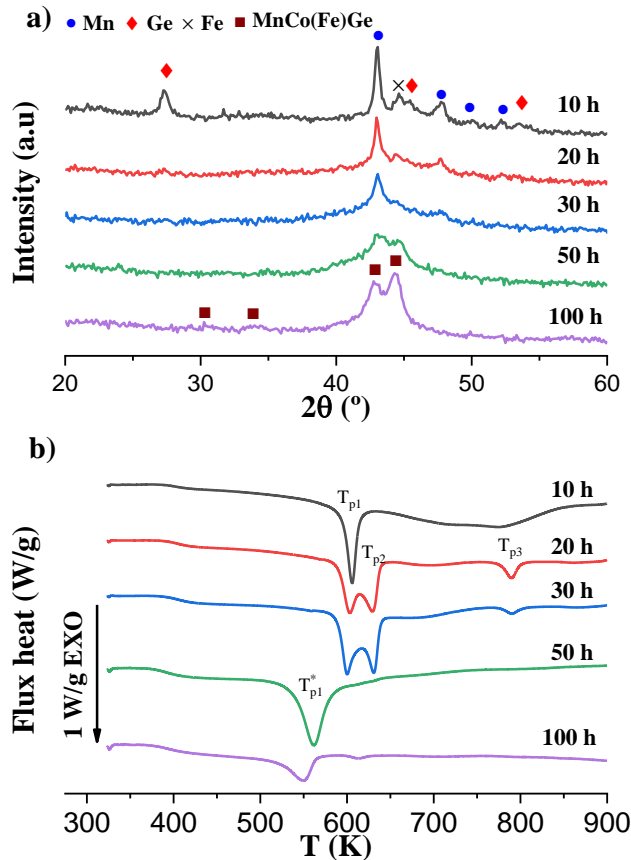
Figure 1. a) XRD patterns of the mechanically alloyed MnCo$_{0.8}$Fe$_{0.2}$Ge powders after different milling times. Symbols indicate the Bragg's positions of each phase. **b)** DSC scans at 20 K/min from room temperature to 973 K as a function of milling time. The arrow indicates the magnitude and nature of the transformation, in this case, all of them are exothermic transformations.

Figure 1 a) shows the evolution of the XRD patterns as a function of the milling time. After 10 h, different starting pure phases are still recognized superimposed to a broad halo, which becomes more evident as milling progresses up to 50 h. This amorphous halo is formed as the evolution of a starting hcp Co phase that rapidly broadens after short milling times [11]. After 100 h milling, new crystalline peaks already detected after 50 h increase indicating a recrystallization process occurred during milling leading to the formation of an intermetallic phase: MnCo(Fe)Ge ($P6_3/mmc$ space group), which is the

4

intermetallic phase of interest in this study. These diffraction maxima were already observed after 50 h milling and quantitative analysis leaded to crystal size < 10 nm for as-milled samples after 50 and 100 h.

Figure 1 b) shows DSC scans at 20 K/min from room temperature to 973 K as a function of milling time. The milling process led to the formation of metastable phases, which transform to more stable ones on heating. This is evidenced in the DSC experiments from the several exothermic transformation processes observed. As it is shown below, XRD patterns on heated samples showed that the stable phase to which the metastable ones transform is the intermetallic MnCoGe-type phase independently of the milling time despite the differences in the DSC exothermic processes. In fact, as milling progresses, the number of exothermic processes and their temperatures changes. After 10 h, there is an exothermic peak at $T_{p1} =$ 606 K with a transformation heat, ΔH = -24 ± 1 J/g. A broad process could be observed at higher temperatures. After 20 h milling, the main peak is subdivided into two peaks at $T_{p1} =$ 603 K and $T_{p2} =$ 630 K, with a total transformation heat, ΔH = -39 ± 1 J/g. Moreover, at $T_{p3} =$ 790 K, a small exothermic appears with a transformation heat, ΔH = -6 ± 1 J/g. After 30 h milling, DSC scan is similar. The main double peak remains. The peak temperatures are nearly constant but the transformation heat increased, ΔH = -43 ± 1 J/g. The high temperature event, at 790 K still appears but its transformation heat decreased, ΔH = -2 ± 1 J/g. After 50 h, the DSC plot changes to a single DSC exothermic shifted to lower temperatures, $T_{p1}{}^* =$ 562 K, with ΔH = -52 ± 1 J/g. After 100 h milling, the recrystallization phenomenon observed from XRD is confirmed and related to a strong decrease of the main peak, ΔH = -17 ± 1 J/g, which slightly shifts to 550 K. A tiny peak appears at 613 K.

Once the thermal stability of the system was determined as a function of milling time, several samples were treated to promote intermetallic phase formation. On the one hand, a conventional annealing taken from literature as appropriate for this type of alloy system [5–7,12–17] was carried out to the sample milled 100 h, which consists in 72 h annealing at 1123 K. On the other hand, low temperature treatments based on DSC results were performed consisting on heating from room temperature up to 723 K at 20 K/min in the calorimeter. This thermal treatment was applied to samples milled at different milling times.

Figure 2 shows the evolution of the XRD patterns of thermally treated samples as a function of the milling time to obtain the precursor system along with the XRD pattern of the conventionally annealed sample. XRD pattern of conventionally annealed sample shows the formation of intermetallic MnCoGe-type phase as the single phase present except for some traces of MnO. As milling time of the precursor increases, the diffraction maxima corresponding to the intermetallic phase become more

evident. However, single phase systems, as observed for the conventionally annealed sample, are only obtained for samples milled 50 h or more.
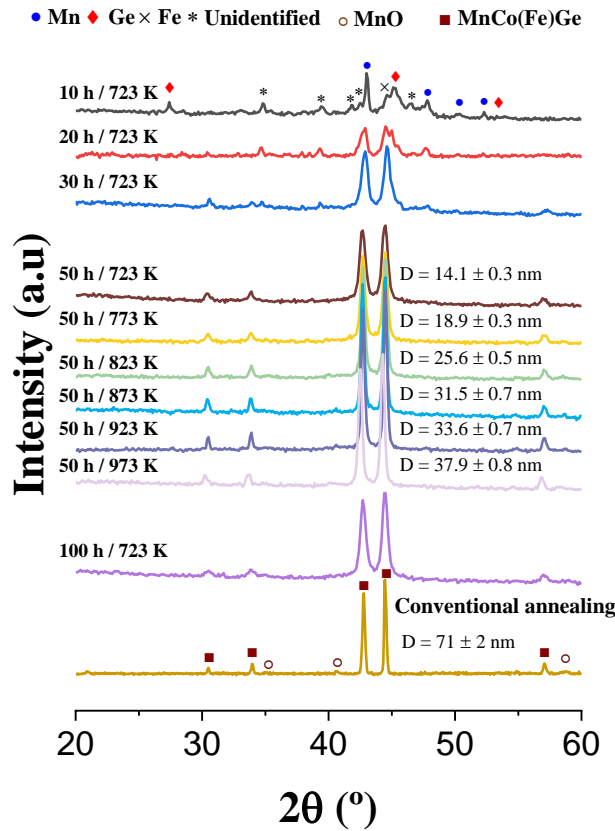

Figure 2. XRD patterns of samples milled for different milling times and heated up to different temperatures at 20 K/min in the calorimeter. The pattern below corresponds to a sample milled 100 h and treated to 1123 K for 72 h in a high temperature furnace in argon (conventional annealing). Symbols indicate the Bragg's positions of intermetallic phase. *D* indicates the crystal size.

Figure 3(a) shows, as an example, the isothermal magnetization curves of the sample milled 50 h and heated up to 723 K at 20 K/min. Figure 3(b) shows, as an example, the temperature dependence of magnetization for the sample milled 50 h and heated up to 723 K. The strong decrease in magnetization is due to the magnetic transition from ferromagnetic to paramagnetic state. The nature of this magnetic transition has been studied using Banerjee criterion [18] which establishes that the slopes of the isotherms in the Arrott plots (H/σ versus σ^2, where σ is the specific magnetization) must be positive in the case of a second order transition, whereas negative slopes are indicative of a first order character of the transition. Figure 3(c) shows the Arrott plots corresponding to the data shown in figure 3(a). According to Banerjee criterion, this sample exhibits a second order phase transition. This character is exhibited by all the samples studied in this work.
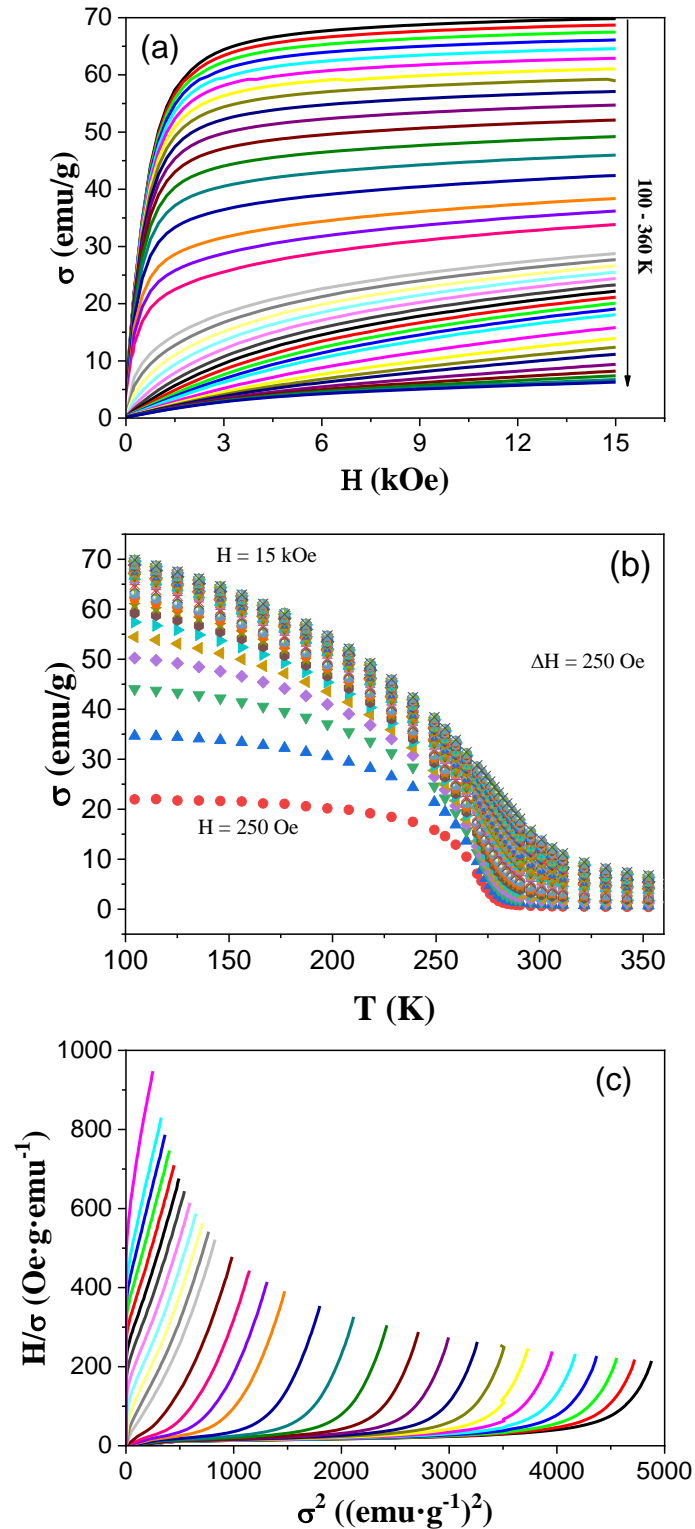
6

Figure 3. Isothermal magnetization curves (a), temperature dependence of magnetization (b), and Arrott plots for sample milled 50 h and heated up to 723 K at 20 K/min.

Figure 4 shows the magnetic entropy change for a maximum field change of $\mu_0 H = 1.5$ T as a function of temperature, for the different samples studied and table 2 collects their main MCE parameters. As milling time increases, $|\Delta S_M|$ increases in clear correspondence with the enhancement of the single phase character of the samples and the development of the intermetallic phase. Concerning the samples submitted to the low temperature treatment, sample obtained from the 50 h milled precursor alloy can be identified as the optimal as far as ΔS_M is close to the maximum value achieved but *RC* is even larger than that of the conventionally annealed sample. Moreover, the obtained values in this study are similar to those reported in the literature for similar compositions [5] rescaling the field change using the power law followed by the magnetic entropy change [19] with a general field exponent of 2/3 characteristic of mean-field second order phase transitions.
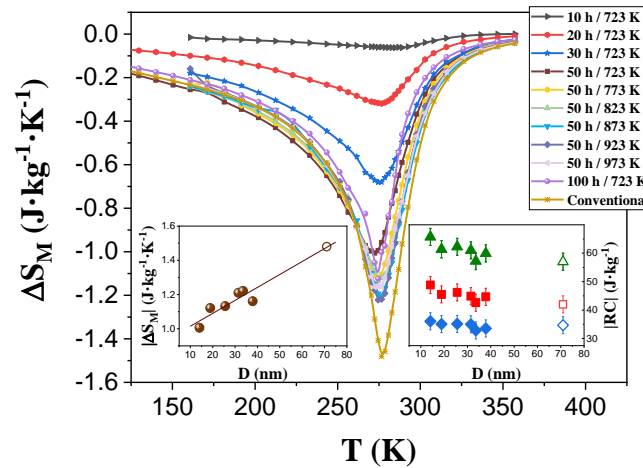

Figure 4. Temperature dependence of ΔS_M as a function of milling time and treatment temperature (heating at 20 K/min). Left inset shows crystal size dependence of maximum $|\Delta S_M|$ and right inset shows the crystal size dependence of *RC* (triangles corresponds to RC_{FWHM}, squares corresponds to RC_{AREA} and diamonds corresponds to RC_{WP}). Empty symbols correspond to the data obtained for conventional annealed sample.

Table 2. MCE response at ΔH=1.5 T as a function of milling time

Milling time (h)	Max ΔS_M ± 0.01 (J·kg^{-1}·K^{-1})	RC_{FWHM} (J·kg^{-1})	T_C ± 3 (K)
10	-0.06	-6 ± 1	275
20	-0.32	-28 ± 1	276
30	-0.68	-49 ± 2	275
50	-1.01	-66 ± 3	272
100	-1.12	-24 ± 1	275
Conventional Annealing	-1.48	-57 ± 3	277

==Both conventional and low temperature annealed samples present a single phase system. Samples submitted to short annealing times are candidates to develop enhanced inhomogeneities with respect to==

long time annealed ones. Recently, we proposed a quantitative method to estimate such inhomogeneities from the evolution of magnetocaloric response and approach to saturation behavior during the transition [20-22]. This method supplies the following equations:

$$T_{inf}^{Weiss} - \langle T_C \rangle = -0.732(6)\Delta T_c \qquad (2)$$

$$T_{MCE}^{Weiss} - \langle T_C \rangle = -0.658(8)\Delta T_c \qquad (3)$$

$$T_{\chi}^{Weiss} - \langle T_C \rangle = 0.503(24)\Delta T_c - 0.0040(7)\Delta T_C^2 \qquad (4)$$

Where T_{inf}^{Weiss}, T_{MCE}^{Weiss} and T_{χ}^{Weiss} are the inflexion point of the zero field saturation magnetization, the peak temperature of the MCE and the peak temperature of the paramagnetic susceptibility and $\langle T_C \rangle$ and ΔT_c are the average Curie temperature and the standard deviation of the Gaussian distribution that describes the inhomogeneous system.

Application of Eq. (2) and (4) or (3) and (4) allows us to estimate $\langle T_C \rangle \sim 285$ K and $\Delta T_c \sim 10$ K for the samples heated at 20 K/min and $\langle T_C \rangle \sim 287$ K and $\Delta T_c \sim 9$ K for conventional annealed sample. The samples heated at 20 K/min points to a broader distribution than conventional annealed sample, which could indicate a greater inhomegeneity in the non isothermally treated samples.

The only significant difference detected is the crystal size (14 and ~70 nm for the low temperature and the conventionally annealed samples, respectively). The large temperature span between both treatments allows us to control this parameter. The XRD patterns of samples obtained from the 50 h milled precursor and heated up to the different temperatures, from 723 to 973 K, at 20 K/min (see Fig.2) show a single intermetallic MnCoGe-type phase, which crystal size increases as treatment temperature increases. There exists a clear and almost linear correlation between the crystal size and maximum $|\Delta S_M|$ for these samples (see Fig.4). Left inset of figure 4 shows this correlation between the crystal size and maximum $|\Delta S_M|$. However, RC decreases as crystal size increases (right inset). This could be related to an enhancement of homogeneity as the heating temperature increases. Therefore, magnetocaloric properties are easily tunable by controling the maximum temperature achived in a heating rate (even preserving the benefits of lower temperature and shorter annealing times) using mechanically alloyed homogeneous systems as precursors.

4. Conclusions

In conclusion, mechanical alloying is shown to be a successful technique reducing time and temperature of the thermal treatment to develop a Mn(Co,Fe)Ge alloy with interesting magnetocaloric response. Heating temperature is reduced from 1123 K (generally used in the literature in a conventional

treatment) to 723 K and annealing time is reduced from 72 h in an isothermal to roughly 20 min, which is the time needed for a ramp at 20 K/min. Moreover, further optimization could be achieved as there is a clear correlation between magnetocaloric properties and crystal size of Mn(Co,Fe)Ge phase.

Data Availability: The raw/processed data required to reproduce these findings cannot be shared at this time as the data also forms part of an ongoing study.

References

[1]   V. Franco, J.S. Blázquez, B. Ingale, A. Conde, The Magnetocaloric Effect and Magnetic Refrigeration Near Room Temperature: Materials and Models, Annu. Rev. Mater. Res. 42 (2012) 305–342. https://doi.org/10.1146/annurev-matsci-062910-100356.

[2]   V. Franco, J.S. Blázquez, J.J. Ipus, J.Y. Law, L.M. Moreno-Ramírez, A. Conde, Magnetocaloric effect: From materials research to refrigeration devices, Prog. Mater. Sci. 93 (2018) 112–232. https://doi.org/10.1016/j.pmatsci.2017.10.005.

[3]   M.E. Wood, W.H. Potter, General analysis of magnetic refrigeration and its optimization using a new concept: maximization of refrigerant capacity, Cryogenics (Guildf). 25 (1985) 667–683. https://doi.org/https://doi.org/10.1016/0011-2275(85)90187-0.

[4]   B. Chapman, the Geopolitics of Rare Earth Elements: Emerging Challenge for U.S. National Security and Economics, J. Self-Governance Manag. Econ. 6 (2017) 50. https://doi.org/10.22381/jsme6220182.

[5]   S. Lin, O. Tegus, E. Brück, W. Dagula, T.J. Gortenmulder, K.H.J. Buschow, Structural and magnetic properties of MnFe1-xCoxGe compounds, IEEE Trans. Magn. 42 (2006) 3776–3778. https://doi.org/10.1109/TMAG.2006.884516.

[6]   G.J. Li, E.K. Liu, H.G. Zhang, Y.J. Zhang, J.L. Chen, W.H. Wang, H.W. Zhang, G.H. Wu, S.Y. Yu, Phase diagram, ferromagnetic martensitic transformation and magnetoresponsive properties of Fe-doped MnCoGe alloys, J. Magn. Magn. Mater. 332 (2013) 146–150. https://doi.org/10.1016/j.jmmm.2012.12.001.

[7]   K. Ozono, Y. Mitsui, R.Y. Umetsu, M. Hiroi, K. Takahashi, K. Koyama, Magnetic and Structural Properties of MnCo1-xFexGe (0 ≤ x ≤ 0.12), AIP Conf. Proc. 1763 (2016) 0–7. https://doi.org/10.1063/1.4961336.

[8]   Y. Wu, M. Wang, S. Lin, L. Chen, W. Song, Y. Sun, J. Lin, P. Tong, K. Zhang, H. Tong, X. Guo, C. Yang, Colossal negative thermal expansion with an extended temperature interval covering room temperature in fine-powdered Mn0.98CoGe, Applied Physics Letters 109 (2016) 241903. http://dx.doi.org/10.1063/1.4972234.

[9]   C. Suryanarayana, Mechanical alloying and milling, Prog. Mater. Sci. 46 (2001) 1–184. https://doi.org/10.1016/S0079-6425(99)00010-9.

[10]   V. Franco, Determination of the Magnetic Entropy Change from Magnetic Measurements : the Importance of the Measurement Protocol, (2014) 1–19. http://www.lakeshore.com/Documents/MagneticEntropyChangefromMagneticMeasurements.pdf.

[11]   Vidal-Crespo, Ipus, Blázquez, Conde, Mechanical Amorphization and Recrystallization of Mn-Co(Fe)-Ge(Si) Compositions, Metals (Basel). 9 (2019) 534. https://doi.org/10.3390/met9050534.

[12]   Z. Guo, H. Qiu, Z. Liu, Effects of the substitution of Cu for Sn on structural, magnetic and magnetocaloric properties of half-Heusler CoMnSn alloy, J. Alloys Compd. 777 (2019) 472–477. https://doi.org/https://doi.org/10.1016/j.jallcom.2018.11.017.

[13]   E. Zubov, N. Nedelko, A. Sivachenko, K. Dyakonov, Y. Tyvanchuk, M. Marzec, V. Valkov, W. Bażela, A. Ślawska-Waniewska, V. Dyakonov, A. Szytuła, H. Szymczak, Influence of replacement of Mn by Cr on

magnetocaloric properties of quenched NiMn1–xCrxGe alloys, Low Temp. Phys. 44 (2018) 775–779. https://doi.org/10.1063/1.5049157.

[14] M. Budzynski, V.I. Valkov, A. V Golovchan, V.I. Kamenev, V.I. Mitsiuk, A.P. Sivachenko, Z. Surowiec, T.M. Tkachenka, Chromium and iron contained half-Heusler MnNiGe-based alloys, J. Magn. Magn. Mater. 396 (2015) 166–168. https://doi.org/https://doi.org/10.1016/j.jmmm.2015.08.052.

[15] S.K. Pal, C. Frommen, S. Kumar, B.C. Hauback, H. Fjellvåg, T.G. Woodcock, K. Nielsch, G. Helgesen, Comparative phase transformation and magnetocaloric effect study of Co and Mn substitution by Cu in MnCoGe compounds, J. Alloys Compd. 775 (2019) 22–29. https://doi.org/https://doi.org/10.1016/j.jallcom.2018.10.040.

[16] C.L. Zhang, Y.G. Nie, H.F. Shi, E.J. Ye, Z.D. Han, D.H. Wang, Tuning magnetostructural transition and the associated giant magnetocaloric effect via thermal treatment in MnCoGe-based alloys, J. Magn. Magn. Mater. 469 (2019) 437–442. https://doi.org/10.1016/j.jmmm.2018.09.016.

[17] S. Yuce, N.M. Bruno, B. Emre, I. Karaman, Accessibility investigation of large magnetic entropy change in CoMn1−xFexGe, J. Appl. Phys. 119 (2016) 133901. https://doi.org/10.1063/1.4945118.

[18] B.K. Banerjee, On a generalised approach to first and second order magnetic transitions, Phys. Lett. 12 (1964) 16–17. https://doi.org/10.1016/0031-9163(64)91158-8.

[19] V. Franco, J.S. Blázquez, A. Conde, Field dependence of the magnetocaloric effect in materials with a second order phase transition: A master curve for the magnetic entropy change, Appl. Phys. Lett. 89 (2006) 9–12. https://doi.org/10.1063/1.2399361.

[20] A.F. Manchón-Gordón, L.M. Moreno-Ramírez, J.J. Ipus, J.S. Blázquez, C.F. Conde, V. Franco, A. Conde, A procedure to obtain the parameters of Curie temperature distribution from thermomagnetic and magnetocaloric data, J. Non. Cryst. Solids. 520 (2019) 119460. https://doi.org/https://doi.org/10.1016/j.jnoncrysol.2019.119460.

[21] A.F. Manchón-Gordón, L.M. Moreno-Ramírez, J.J. Ipus, J.S. Blázquez, C.F. Conde, V. Franco, A. Conde, Correction to "A procedure to obtain the parameters of curie temperature distribution from thermomagnetic and magnetocaloric data" orginally published as J. non-cryst. solids 520, 119,460 (2019), J. Non. Cryst. Solids. 538 (2020) 120047. https://doi.org/https://doi.org/10.1016/j.jnoncrysol.2020.120047.

[22] A.F. Manchón-Gordón, R. López-Martín, A. Vidal-Crespo, J.J. Ipus, J.S. Blázquez, C.F. Conde, A. Conde, Distribution of Transition Temperatures in Magnetic Transformations: Sources, Effects and Procedures to Extract Information from Experimental Data, Metals (Basel). 10 (2020) 226. https://doi.org/10.3390/met10020226.